THE ASTRONOMICAL JOURNAL, 121:1266–1274, 2001 March

GALAXY MORPHOLOGICAL SEGREGATION IN CLUSTERS: LOCAL VERSUS GLOBAL CONDITIONS

MARIANO DOMÍNGUEZ, HERNÁN MURIEL, AND DIEGO G. LAMBAS
Grupo de Investigaciones en Astronomía Teórica y Experimental, Observatorio Astronómico de Córdoba, Laprida 854, 5000 Córdoba, Argentina, and CONICET, Buenos Aires, Argentina; mardom@oac.uncor.edu, hernan@oac.uncor.edu, dgl@oac.uncor.edu
Received 2000 September 29; accepted 2000 November 6

ABSTRACT

We study the relative fraction of galaxy morphological types in clusters as a function of the projected local galaxy density and of different global parameters: cluster projected gas density, cluster projected total mass density, and reduced cluster-centric distance. Since local and global densities are correlated, we have considered different tests to search for the parameters on which segregation shows the strongest dependence. We have also explored the results of our analysis as they apply to both the central regions of the clusters and their outskirts. We consider a sample of clusters of galaxies with estimated temperatures and derive the projected mass density profile, using the model of Navarro, Frenk, & White, and the 500 overdensity contrast radius (r_{500}), using the scaling relation. X-ray surface brightness profiles are used to obtain the projected gas density, assuming the hydrostatic equilibrium model. Our results suggest that morphological segregation in clusters is controlled by local galaxy density in the outskirts. On the other hand, global projected mass density shows the strongest correlation with the fractions of morphological types in the central high-density region, with a marginal dependence on local galaxy density.

Key words: galaxies: clusters: general — galaxies: evolution — galaxies: fundamental parameters — intergalactic medium — X-rays

1. INTRODUCTION

The difference between the population of galaxies in the field and in clusters has been well known since the early 1930s. Oemler (1974) analyzed the proportions of elliptical, S0, and spiral galaxies and defined three types of clusters: spiral-rich, spiral-poor, and cD. Melnick & Sargent (1977) showed that the inner regions of clusters are typically populated by elliptical galaxies and that spirals are predominant in the outer regions (the well-known morphological segregation).

In a classic work, Dressler (1980b) analyzed a sample of 55 nearby clusters, finding a correlation between the fractions of different morphological types, T, and the local projected galaxy density, Σ (hereafter the T-Σ relation). Dressler concluded that galaxy morphology is a function of local clustering rather than of global conditions related to the cluster environment.

Sanromà & Salvador-Solé (1990) have considered a test to explore the nature of morphological segregation. Using Dressler's data, they generated artificial clusters by randomly repositioning the polar coordinates of galaxy members around the centers of the clusters. In this way any subclustering is erased, maintaining the radial cluster-centric distance of each galaxy so that the global cluster properties are conserved. The T-Σ relation for the randomized galaxies in the clusters was analyzed and compared with that based on the real galaxy positions. The results were indistinguishable, indicating that the T-Σ relation is controlled by global conditions rather than local subclustering.

Whitmore & Gilmore (1991) and Whitmore, Gilmore, & Jones (1993, hereafter WGJ) reexamined Dressler's sample of galaxies in clusters and suggested that the morphology–cluster-centric distance relation is more fundamental than the morphology–local galaxy density relation. These authors use the cluster-centric normalized distance as the independent parameter and compare the morphological fractions at the same normalized cluster-centric radii with different values for local galaxy density. WGJ use a "characteristic radius," $r_{\rm opt}$, as the radius at which the cumulative projected galaxy density falls below 20 galaxies Mpc^{-2}. These authors find that for small radii (about 0.5 Mpc) the elliptical fraction rises rapidly. On the other hand, the spiral fraction is essentially zero at the cluster center. WGJ interpret these results as an indication that cluster center conditions play a key role in determining galaxy morphologies in clusters and suggest that a destructive rather than a formation mechanism may be controlling their relative fractions.

The question whether local galaxy density or radial distance from the cluster center is better correlated with morphological types is still open. Dressler et al. (1997, hereafter D97) reanalyzed the morphology-density relation by dividing their sample into centrally concentrated, regular clusters and low-concentration, irregular clusters, finding a similar T-Σ relation in both subsamples. Nevertheless, they found a significant excess of S0's and a smaller spiral fraction in centrally concentrated clusters than in low-concentration systems.

D97 also analyzed a sample of 10 clusters at redshifts between 0.37 and 0.56 and derived the corresponding T-Σ relation. For these distant clusters the authors found that the fraction of S0 galaxies is 2–3 times smaller than in low-redshift clusters, suggesting that S0's are generated in large numbers only after cluster virialization. It should be recalled, however, that an artificial increase of the late-type fraction in distant clusters may be caused by the possibility of systematic effects related to projection biases in the selection of clusters from two-dimensional data (see, e.g., Valotto, Moore, & Lambas, 2001).

Several mechanisms have been proposed in order to explain morphological segregation. Among them we can mention ram pressure stripping (Gunn & Gott 1972; Abadi, Moore, & Bower 1999), gas evaporation (Cowie & Songaila 1977), merging (Lavery & Henry 1988), galaxy harassment

(Moore et al. 1996), tidal stripping (galaxy-galaxy and from mean cluster field; Byrd & Valtonen 1990), tidal shaking (galaxy-galaxy and from mean cluster field; Miller 1988), galactic cannibalism (Ostriker & Tremaine 1975), and truncated star formation (Larson, Tinsley, & Caldwell 1980). Also to be considered are the effects of the initial conditions, which may also play a role in morphological segregation. In hierarchical models of structure formation, such as cold dark matter, different scales become nonlinear simultaneously, so that the initial conditions of galaxy formation in cluster and group environments may differ from those in the field (intergalactic medium, tidal effects, mergers, etc.).

In this work, we study the relative fraction of galaxy morphologies in clusters as a function of global cluster parameters (projected mass and gas density profile), and of local projected galaxy density. Our analysis is aimed at providing a better understanding of the relevance of the proposed mechanisms involved in morphological segregation in clusters, given their different dependence on gas, mass, and galaxy content.

The paper is organized as follows: In § 2, we briefly review the data used for this study. In § 3, we explore morphological segregation as a function of different global and local parameters and perform a simple test to compare their relative importance. Section 4 provides a discussion of the main results and some implications for galaxy evolution in clusters. We include in the Appendix a short discussion on the corrections applied to deal with observational biases.

2. DATA

The data are drawn from clusters originally analyzed by Dressler (1980a). That survey provides morphological determination for $\sim$6000 galaxies in 55 nearby clusters. From this sample we have selected a subsample of 22 rich clusters (see Table 1) with estimated (or measured) gas temperatures and X-ray surface brightness information. From the Jones & Forman (1999) analysis of *Einstein* X-ray images we obtain the central gas density ρ_0, the core radius r_c, and the β-parameter for each cluster in our sample. Temperatures are taken from different sources in the literature, and as Table 1 illustrates, our sample comprises a wide range of temperatures, from poor cluster environments ($\sim$1.5 keV) to massive clusters ($\sim$8 keV). Cluster center coordinates in Table 1 correspond to the maxima of X-ray emission. We have excluded clusters with peculiarities in their X-ray luminosity distribution, such as double clusters consisting of two substructures of comparable size and luminosity and objects with a significant presence of substructure or strong departures from sphericity.

3. METHODS AND ANALYSIS

In this section we explore the dependence of the relative fraction of galaxy morphological types in clusters on the local galaxy environment, namely, the projected local galaxy density as defined by Dressler (1980b), and on a variety of global parameters: cluster projected total mass density and gas density, and two different reduced cluster-centric distances.

3.1. *Local Galaxy Density*

In order to assess the relevance of local processes that may affect galaxy morphology, we compute the relative fraction of galaxy morphologies as a function of the project-

TABLE 1

CLUSTER SAMPLE

Name (1)	R.A. (B1950.0) (2)	Decl. (B1950.0) (3)	z (4)	T_X (keV) (5)	r_c (Mpc) (6)	β (7)	ρ_0 (10^{-3} cm^{-3}) (8)	r_{opt} (Mpc) (9)	r_{500} (Mpc) (10)
A0076	00 37 25.1	+06 33 32	0.0416	1.5	0.41	0.60	0.522	0.23	0.90
A0119	00 53 43.5	−01 31 28	0.0440	5.9	0.32	0.53	1.221	0.83	1.79
A0154	01 08 22.2	+17 23 37	0.0658	3.1	0.17	0.55	1.690	0.80	1.25
A0194	01 23 20.0	−01 38 12	0.0178	1.4	0.20	0.60	0.719	0.38	0.90
A0376	02 42 57.3	+36 41 52	0.0488	5.1	0.08	0.46	3.941	1.05	1.65
A0400	02 55 00.0	+05 48 25	0.0232	2.5	0.26	0.65	4.430	0.43	1.20
A0496	04 31 20.4	−13 21 48	0.0320	3.9	0.14	0.59	5.283	0.39	1.48
A0539	05 13 55.2	+06 23 16	0.0205	3.0	0.11	0.60	3.054	0.56	1.32
A0592	07 39 56.5	+09 29 30	0.0624	3.2	0.14	0.60	2.606	0.26	1.28
A0957	10 11 07.9	−00 40 53	0.0440	2.8	0.14	0.52	1.720	0.56	1.23
A1142	10 58 17.7	+10 47 40	0.0353	3.7	0.19	0.60	0.786	0.28	1.43
A1185	11 08 03.0	+28 59 04	0.0304	3.9	0.15	0.62	1.445	0.39	1.48
A1377	11 44 40.6	+55 59 40	0.0509	2.7	0.29	0.60	0.793	0.42	1.20
A1656	12 57 18.3	+28 12 22	0.0235	8.1	0.43	0.67	2.275	1.24	2.16
A1913	14 24 25.5	+16 53 40	0.0533	2.9	0.57	0.60	0.396	0.61	1.24
A1983	14 50 36.8	+16 55 02	0.0458	2.2	0.08	0.60	3.838	0.60	1.09
A1991	14 52 13.4	+18 50 56	0.0586	5.4	0.06	0.56	10.810	0.25	1.67
A2040	15 10 21.0	+07 37 06	0.0456	2.5	0.14	0.60	1.782	0.48	1.16
A2256	17 06 44.3	+78 42 46	0.0601	7.5	0.58	0.76	1.278	1.05	1.97
A2634	23 35 54.9	+26 44 19	0.0312	3.4	0.42	0.60	0.597	0.98	1.38
A2657	23 42 22.9	+08 54 15	0.0414	3.4	0.14	0.52	3.018	0.73	1.36
Centaurus.....	12 46 03.4	−41 02 26	0.0107	3.9	0.15	0.45	1.939	...	1.52

NOTES.—Units of right ascension are hours, minutes, and seconds, and units of declination are degrees, arcminutes, and arcseconds. Col. (4): cluster redshift; col. (5): cluster temperature; col. (6): core radius; col. (7): β-parameter; col. (8): central density; col. (9): optical core radius; col. (10): 500 overdensity radius.

ed local galaxy density in the same way as D97. We define the local galaxy density Σ_{gal} for each galaxy in our sample using the same procedure as D97. We compute the rectangular area that comprises the 10 nearest galaxies around each object and correct for completeness in luminosity and contamination from projections using methods described by WGJ and discussed in the Appendix. Figure 1 shows the results, which are similar to those given by D97, indicating that our subsample of X-ray clusters is representative of optically selected galaxy systems. Errors bars in all figures in this paper were computed using the bootstrap resampling technique (Barrow, Bhavsar, & Sonoda 1984).

3.2. *Projected Cluster Mass Density*

The effect of the global cluster environment on galaxy morphology requires the computation of parameters that quantify the effects of the cluster as a whole on each galaxy. It is important to consider the total mass density of clusters, given its relevance to several of the processes (e.g., cluster tidal field) that could affect galaxy morphology.

Navarro, Frenk, & White (1995, hereafter NFW) have proposed an analytic universal density profile of dark matter halos based on numerical simulations and analytical models, assuming spherical symmetry and accretion onto an initially overdense perturbation. The NFW fitting function,

$$\rho(x) = \rho_s/[x(1+x)^2] , \quad x = r/r_{\delta_c} , \tag{1}$$

describes cluster mass density profiles, where r_{δ_c} is the radius corresponding to a mean overdensity δ_c. This function has the advantage that the dark matter halos can be described with a single parameter over a broad rage of halo masses. Based on numerical simulations, Evrard, Metzler, & Navarro (1996) predict that the average cluster temperature T_X strongly correlates with r_{δ_c} and propose the following relation:

$$r_{\delta_c}(T_X) = r_{10}(\delta_c)[T_X/(10\ \mathrm{keV})] . \tag{2}$$

The normalization $r_{10}(\delta_c)$ corresponds to the radial scale of 10 keV clusters at density contrast δ_c (2.48 Mpc), and we adopt a standard overdensity parameter $\delta_c = 500$.

Bartelmann (1996) has derived the projected mass density (Σ_{mass}) profile corresponding to the NFW function:

$$\Sigma_{mass}(x) = \frac{2\rho_s r_{\delta_c}}{x^2 - 1} f(x) , \tag{3}$$

where

$$f(x) = \begin{cases} 1 - \dfrac{2}{\sqrt{x^2-1}} \operatorname{arctanh} \sqrt{\dfrac{x-1}{x+1}} , & \text{if } x > 1 , \\ 1 - \dfrac{2}{\sqrt{1-x^2}} \operatorname{arctanh} \sqrt{\dfrac{1-x}{1+x}} , & \text{if } x < 1 , \\ 0 , & \text{if } x = 1 . \end{cases}$$

We adopt the mean cluster temperatures quoted in Table 1 in equation (2) to derive r_{500}. The projected mass density Σ_{mass} at the position of each galaxy can then be obtained by equation (3).

For all clusters we compute the relative fraction of morphological types in bins of Σ_{mass}. The results are shown in Figure 2, where a very significant dependence of these fractions on the local mass density inferred from the projected NFW profile can be appreciated.

Local versus global effects might be reflected in the differing dependence of the morphological segregation on Σ_{gal} and Σ_{mass}. By comparing Figures 1 and 2, it can be appreciated that both Σ_{mass} and Σ_{gal} provide a good correlation with the relative fraction of morphological types. However, given the correlation between these two densities, as shown

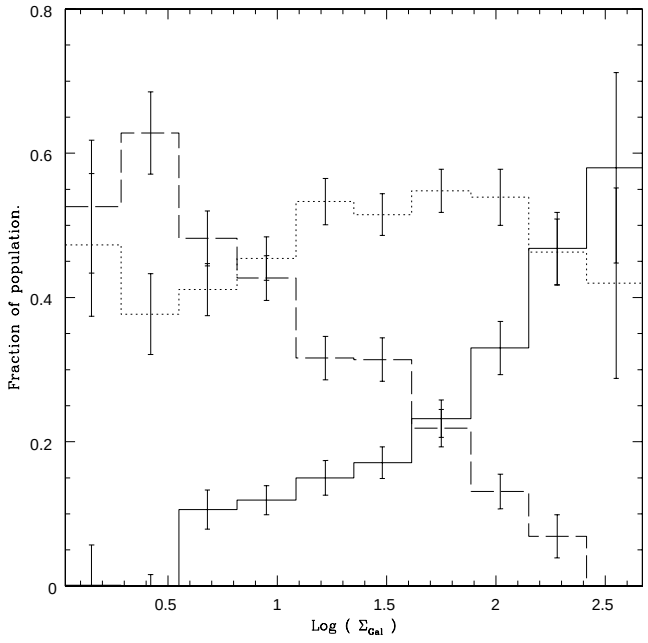

FIG. 1.—Relative fraction of E (*solid line*), S0 (*dotted line*), and S+I (*dashed line*) galaxies as a function of the local galaxy density.

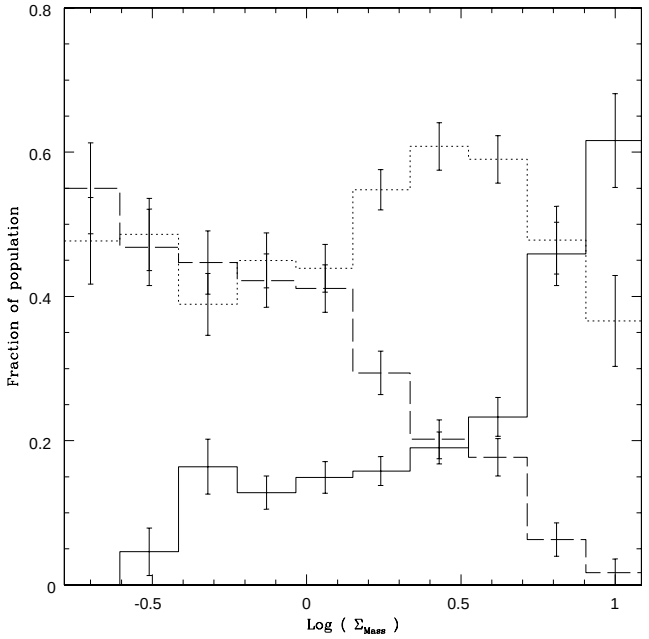

FIG. 2.—Same as Fig. 1, but for the projected mass density

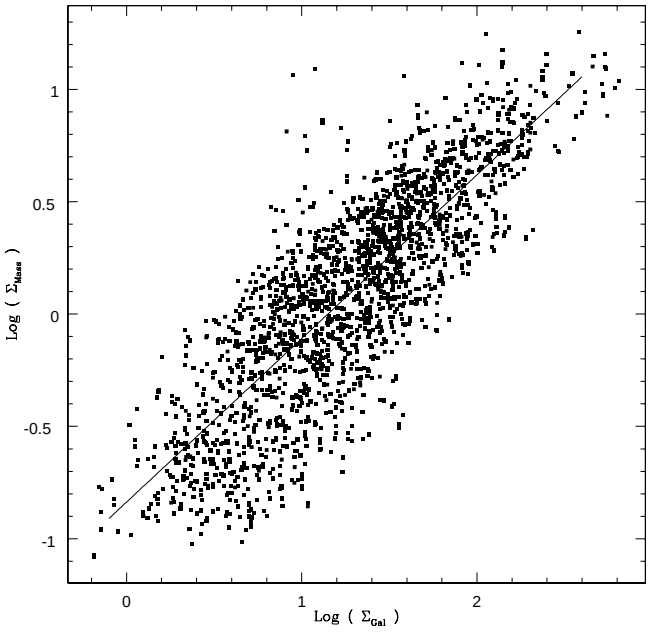

FIG. 3.—Correlation between local galaxy density Σ_{gal} and projected cluster mass density Σ_{gas} at the position of each galaxy of the cluster sample. The solid line corresponds to the best power-law fit.

in Figure 3, it is important to analyze whether they are primary or secondary parameters in the morphological segregation. In order to address this point, we consider for simplicity two morphological groups, early (elliptical and S0) and late (spiral and irregular) types, in the following tests: (1) Our galaxy sample is divided according to Σ_{gal} for bins of Σ_{mass}. For each bin of Σ_{mass} we divide our sample into three equal subsamples: low, intermediate, and high Σ_{gal}. For the high and low projected galaxy density subsamples we compute the fraction of early and late types as a function of the global mass density (in the position of each object). The results of this test are displayed in Figures 4*a* and 4*b*. (2) We divide our galaxy sample according to Σ_{mass} for bins of Σ_{gal}. For each bin of Σ_{gal} we divide our sample into three equal subsamples: low, intermediate, and high Σ_{mass}. For the high and low projected mass density subsamples we compute the fraction of early and late types as a function of the local galaxy density. The results of this second test are shown in Figures 4*c* and 4*d*.

It should be recalled that the results shown in Figures 4*a* and 4*b* show significant differences in the fraction of morphological types between the high- and low-Σ_{gal} subsamples at low values of Σ_{mass}, i.e., typically in the outskirts of the clusters. On the other hand, Figures 4*c* and 4*d* show signifi-

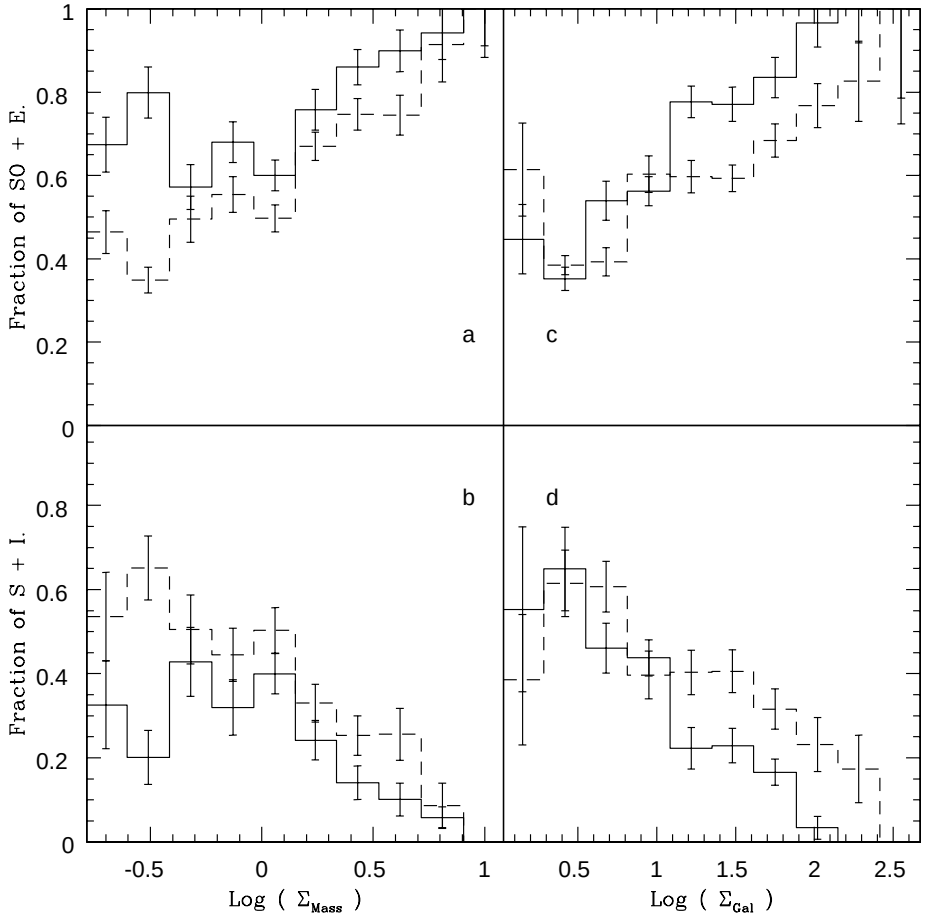

FIG. 4.—Relative fraction of galaxy morphological types as a function of the global projected mass density Σ_{mass} and local galaxy density Σ_{gal}. (*a*) Fraction of E+S0 galaxies vs. Σ_{mass} at high (*solid line*) and low (*dashed line*) Σ_{gal}. (*b*) Same as (*a*), but for the relative fraction of S+I galaxies. (*c*) Fraction of E+S0 galaxies vs. Σ_{gal} at high (*solid line*) and low (*dashed line*) Σ_{mass}. (*d*) Same as (*c*), but for the relative fraction of S+I galaxies.

cant differences in the relative fraction of early and late types between the high- and low-$\Sigma_{\rm mass}$ subsamples at high values of $\Sigma_{\rm gal}$, i.e., in the central virialized regions of clusters. In order to provide a quantitative measurement of these effects we have computed the differences in the relative fraction of morphological types for the high- and low-density subsamples. We sum these differences and compute the corresponding averages and dispersions across the different bins in total range of densities (see Table 2).

Given the marked difference between the inner and outer regions of the clusters, we have adopted the associated threshold densities $\log \Sigma_{\rm mass} \approx -0.03$ and $\log \Sigma_{\rm gal} \approx 1.1$, which define the low- and high-density samples for tests summarized in Table 2. These values correspond on average to a mean overdensity (δ_c) of 500, a conservative estimate of the boundary between the inner, virialized regions of the clusters and their recently accreted, still-settling outer envelopes, as discussed by Evrard et al. (1996). The results of tests 1 and 2 can be appreciated by inspecting Table 2, where the average differences in morphological fractions, dispersions, and statistical significance, as well as the percentages of galaxies used in each computation, are listed.

These results strongly suggest that local galaxy density should not be considered as the unique parameter that determines the relative fractions of galaxy morphologies in clusters of galaxies. In the outskirts of clusters (the low-density subsamples in tests 1 and 2), $\Sigma_{\rm gal}$ accounts for most of the effect while $\Sigma_{\rm mass}$ may be considered a primary parameter in the high-density virialized region of clusters.

3.3. *Gas Density Profile*

Another global parameter worth considering is the intracluster gas density, which may induce important morphological transformations in galaxies orbiting in the cluster, such as ram pressure processes or gas evaporation. For an isothermal gas distribution in hydrostatic equilibrium, the gas density profile can be obtained by fitting the X-ray surface brightness distribution with the well-known β-model,

$$I_{\rm X} = I_0[1 + (r/r_c)^2]^{-3\beta+1/2} . \quad (4)$$

Fitting β and r_c from the previous equation, the gas density can be derived in this way:

$$\rho_{\rm gas} = \rho_0[1 + (r/r_c)^2]^{-3\beta/2} . \quad (5)$$

This equation can be projected in order to derive the projected intracluster gas density:

$$\Sigma_{\rm gas}(r) = \rho_0 r_c[1 + (r/r_c)^2]^{(1-3\beta_f)/2} B\left(\frac{1}{2}, \frac{3\beta_f - 1}{2}\right), \quad (6a)$$

where

$$B(x, y) = \frac{\Gamma(x)\Gamma(y)}{\Gamma(x + y)} \quad (6b)$$

(M. G. Abadi & J. F. Navarro 2000, private communication). We have computed the fraction of galaxies by morphological types as a function of $\Sigma_{\rm gas}$ for our sample. The results of this correlation are displayed in Figure 5.

We have applied tests similar to those described in the previous section with $\Sigma_{\rm gas}$ and $\Sigma_{\rm gal}$. Now we divide our galaxy sample according to $\Sigma_{\rm gal}$ for bins of $\Sigma_{\rm gas}$. For each bin of $\Sigma_{\rm gas}$ we consider three equal subsamples (low, intermediate, and high $\Sigma_{\rm gal}$) and compute the fraction of mor-

TABLE 2

RESULTS

Parameter	Total	Outskirts (Low Density)	Central Region (High Density)
Test 1:			
Average difference.....	0.12 ± 0.03 (4.6)	0.20 ± 0.06 (3.3)	0.07 ± 0.02 (3.1)
Percentage used	...	37	63
Test 2:			
Average difference.....	0.09 ± 0.03 (3.0)	−0.01 ± 0.07 (0.2)	0.16 ± 0.03 (5.3)
Percentage used	...	40	60
Test 3:			
Average difference.....	0.12 ± 0.03 (4.4)	0.07 ± 0.04 (1.9)	0.13 ± 0.03 (4.8)
Percentage used	...	37	63
Test 4:			
Average difference.....	0.06 ± 0.03 (2.0)	−0.01 ± 0.07 (0.1)	0.11 ± 0.03 (5.1)
Percentage used	...	49	51
Test 5:			
Average difference.....	0.16 ± 0.04 (4.3)	0.24 ± 0.07 (3.2)	0.10 ± 0.03 (2.9)
Percentage used	...	41	59
Test 6:			
Average difference.....	−0.09 ± 0.03 (3.0)	−0.10 ± 0.07 (1.4)	−0.08 ± 0.02 (3.4)
Percentage used	...	47	53
Test 7:			
Average difference.....	0.12 ± 0.03 (4.0)	0.13 ± 0.06 (2.1)	0.10 ± 0.03 (3.1)
Percentage used	...	45	55
Test 8:			
Average difference.....	−0.04 ± 0.03 (1.0)	0.03 ± 0.08 (0.4)	−0.08 ± 0.03 (2.6)
Percentage used	...	42	58

NOTE.—Values in parentheses are the statistical significance of the average difference in morphological fraction.

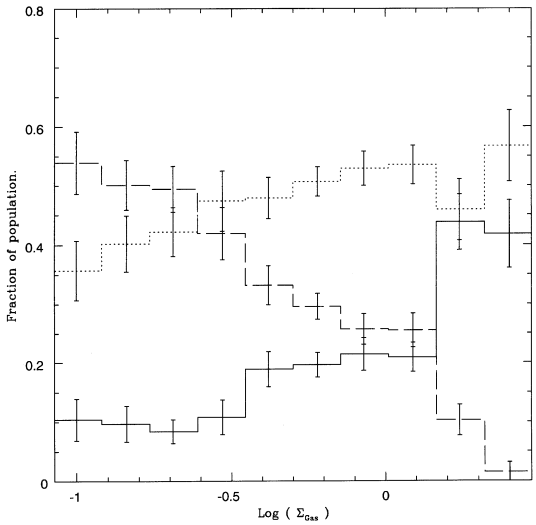

FIG. 5.—Same as Fig. 1, but for the projected gas density

phological types of galaxies as a function of the projected gas density for the high and low galaxy density subsamples (test 3). In a similar way we perform the complementary test for bins of Σ_{gal} and subsamples of Σ_{gas} (test 4). The results of these tests are displayed in Figure 6 and are also summarized in Table 2.

From the results of comparing the mass and gas projected profiles (Figs. 4 and 6 and Table 2) with the local galaxy density, we can infer that the distribution of morphological types shows a stronger correlation with the NFW profile than with the β-model profile.

3.4. *Dependence on Cluster-centric Distances Normalized to r_{opt} and r_{500}*

A standard way to analyze the dependence of galaxy morphology on global cluster parameters is to compute galaxy cluster-centric distances normalized to a cluster characteristic radius.

WGJ have reexamined the relative fractions of galaxy morphological types in Dressler's sample of clusters, concluding that the cluster-centric radial distance is a primary parameter in the morphology segregation and that the local galaxy density, in contrast, is a secondary parameter. We have applied tests similar to those described in the previous sections, and for this case our analysis is equivalent to that of WGJ.

We divide our galaxy sample according to Σ_{gal} for bins of r/r_{opt}, and for each bin in r/r_{opt} we consider three equal subsamples: low, intermediate, and high Σ_{gal}. We compute the fraction of morphological types as a function of r/r_{opt} for the high and low local galaxy density subsamples (test 5). In a similar way we perform the complementary test for bins of

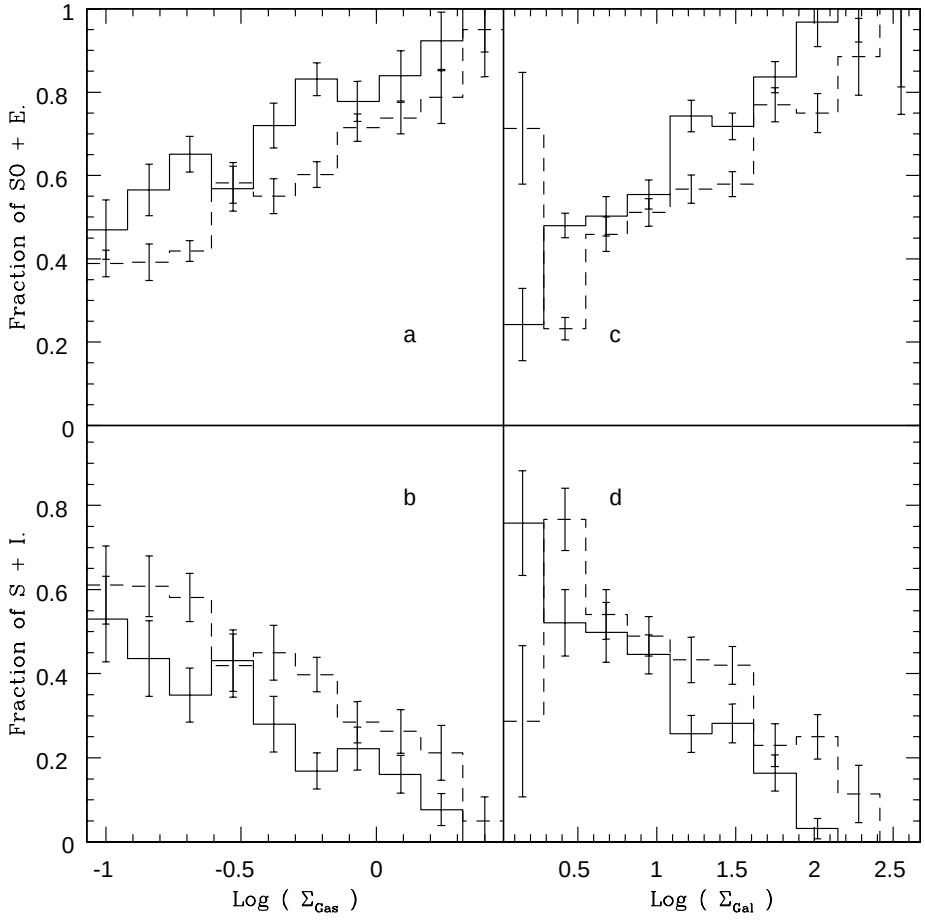

FIG. 6.—Relative fraction of galaxy morphological types as a function of the global projected gas density Σ_{gas} and local galaxy density Σ_{gal}. (*a*) Fraction of E+S0 galaxies vs. Σ_{gas} at high (*solid line*) and low (*dashed line*) Σ_{gal}. (*b*) Same as (*a*), but for the relative fraction of S+I galaxies. (*c*) Fraction of E+S0 galaxies vs. Σ_{gal} at high (*solid line*) and low (*dashed line*) Σ_{gas}. (*d*) Same as (*c*), but for the relative fraction of S+I galaxies.

Σ_{gal} and subsamples of high and low normalized radial distance (test 6).

The results of these tests are shown in Figure 7 and displayed in Table 2. It can be seen that neither Σ_{gal} nor r/r_{opt} can be considered as a primary parameter defining the relation between galaxy morphology and environment. The conclusion from a similar analysis by WGJ applied to the very central regions (within $r/r_{opt} = 0.25$, $\simeq 0.15$ Mpc on average for our sample) is that a normalized cluster-centric distance r/r_{opt} acts as a single parameter driving the galaxy morphological segregation. This is consistent with our results in the first two bins of Figures 7*a* and 7*b*, which correspond to these scales. These figures also illustrate the significant dependence of the relative fractions of galaxy morphologies on Σ_{gal} at larger distances from the cluster centers.

Several works use r_{200} or r_{500} as a characteristic cluster radius (see, e.g., Yee, Ellingson, & Carlberg 1996) in order to make a proper comparison of clusters. In this subsection we adopt the r_{500} radius to normalize each galaxy radial distance, and we apply tests similar to those described above. The results of tests 7 and 8 are displayed in Figure 8 (see also Table 2). From these results we conclude that the dependence of galaxy morphology relative fractions on r/r_{500} is similar to that on r/r_{opt}. Nevertheless, we find these dependencies considerably less significant than that on the NFW projected mass density profile, as can be seen by comparing Figures 4 and 8.

3.5. *Morphological Segregation in Clusters with Low/High X-Ray Luminosity and Intracluster Gas Temperature*

Different authors have analyzed possible dependencies of the morphological segregation on X-Ray luminosity. Dressler (1980b) computed the T-Σ relationship for eight strong X-ray emitters ($L_X \geq 10^{44}$ ergs s^{-1}), finding it similar to that for the total sample. WGJ divided a sample of 39 clusters with X-ray luminosity into three subsamples and found that the morphological fractions as a function of cluster-centric radius had no significant dependence on the cluster X-ray luminosity. X-ray luminosities and intracluster gas temperatures are available for all clusters in our sample. In order to explore the correlations between the distribution of morphological types and global and local parameters of different cluster environments, we have divided our sample into high and low cluster temperature and luminosity subsamples. In a way similar to tests 1–8 above, we computed the fraction of spiral galaxies for high and low Σ_{mass} and Σ_{gal} values in bins of Σ_{gal} and Σ_{mass}, respectively, for two subsamples of clusters, high-luminosity ($L_X \geq 1.638 \times 10^{44}$ ergs s^{-1}) and low-luminosity ($L_X \leq 1.123 \times 10^{44}$ ergs s^{-1}).We have also applied the same analysis to the two subsamples of hot ($T_X \geq 3.7$ keV) and cold ($T_X \leq 3.4$ keV)

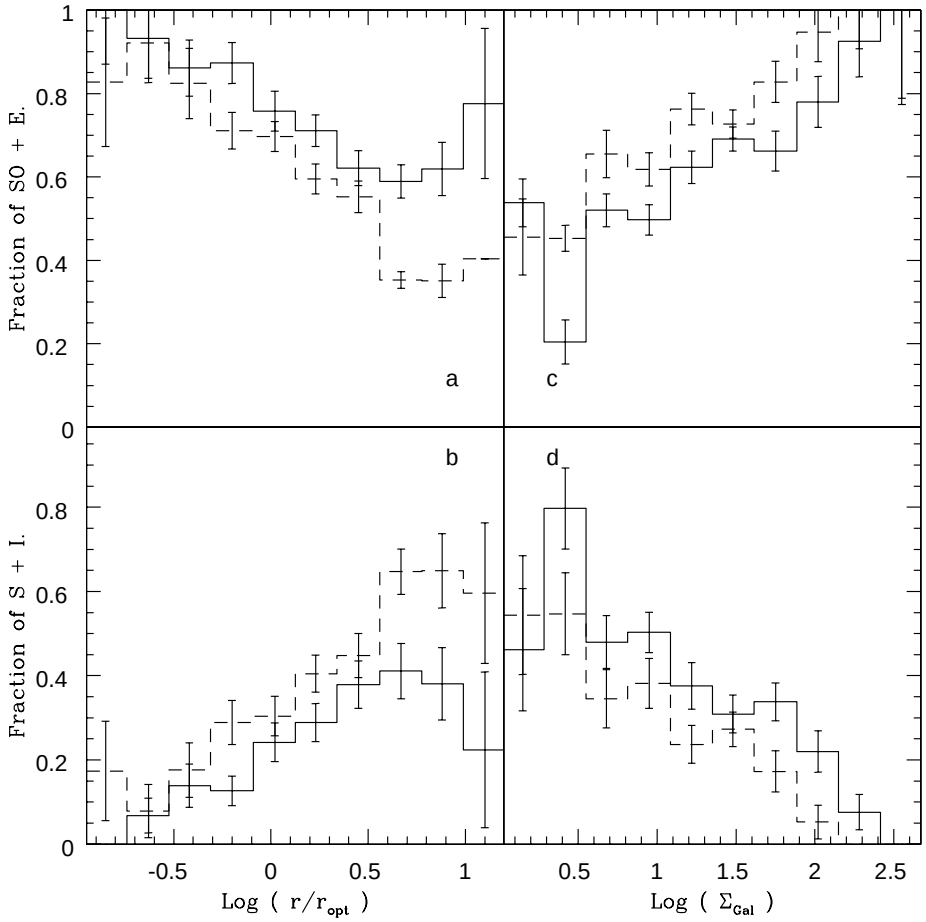

FIG. 7.—Relative fraction of galaxy morphological types as a function of the cluster-centric projected radial distance normalized to r_{opt} and local galaxy density Σ_{gal}. (*a*) Fraction of E + S0 galaxies vs. r/r_{opt} at high (*solid line*) and low (*dashed line*) Σ_{gal}. (*b*) Same as (*a*), but for the relative fraction of S + I galaxies. (*c*) Fraction of E + S0 galaxies vs. Σ_{gal} at high (*solid line*) and low (*dashed line*) r/r_{opt}. (*d*) Same as (*c*), but for the relative fraction of S + I galaxies.

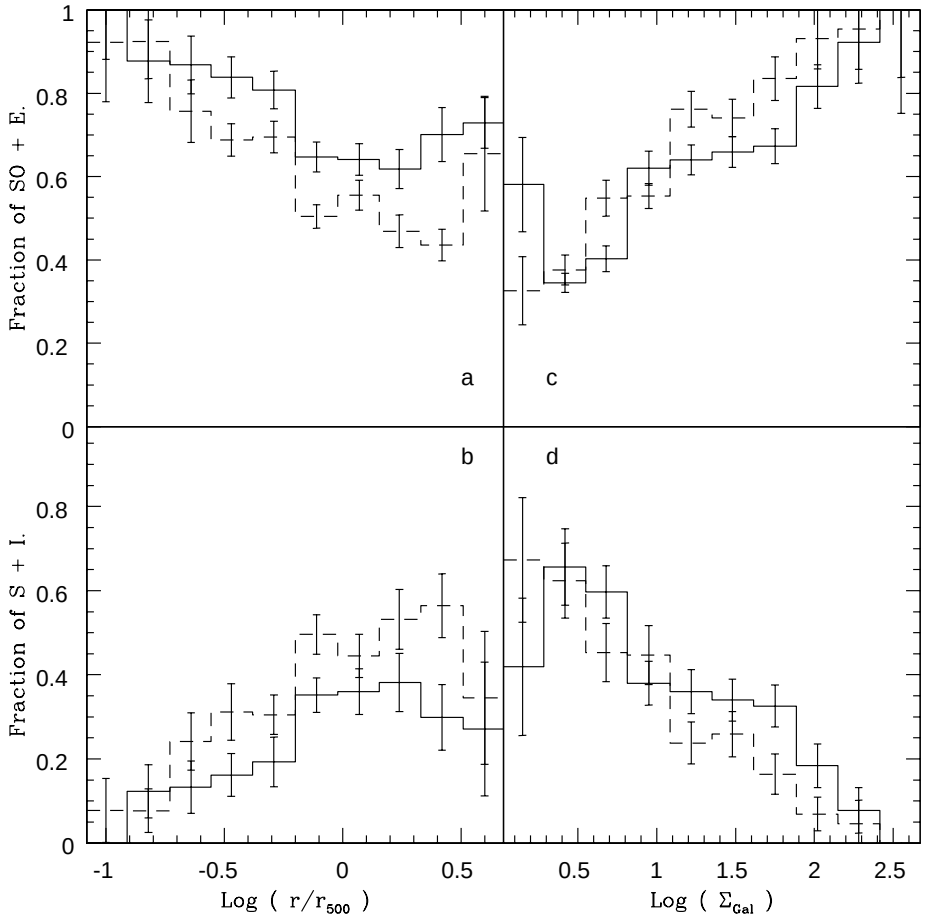

FIG. 8.—Relative fraction of galaxy morphological types as a function of the cluster-centric projected radial distance normalized to r_{500} and local galaxy density Σ_{gal}. (*a*) Fraction of E+S0 galaxies vs. r/r_{500} at high (*solid line*) and low (*dashed line*) Σ_{gal}. (*b*) Same as (*a*), but for the relative fraction of S+I galaxies. (*c*) Fraction of E+S0 galaxies vs. Σ_{gal} at high (*solid line*) and low (*dashed line*) r/r_{500}. (*d*) Same as (*c*) for the relative fraction of S+I galaxies.

clusters. The results of these tests show the lack of a strong dependence on luminosity and temperature, in agreement with Dressler (1980b) and WGJ. However, we note a stronger dependence of the relative morphological fractions on the global mass density versus the local galaxy density in the central regions of the high-temperature and high-luminosity subsamples than in the low-temperature, low-luminosity subsamples.

4. DISCUSSION AND CONCLUSIONS

In hierarchical scenarios for structure formation in the universe, clusters are assembled from smaller units, so that the local galaxy density associated with these primordial clumps could play a significant role in the segregation of morphological types. On the other hand, several mechanisms related to galaxy evolution within the potential well of clusters (ram pressure, tidal effects, etc.) could also explain the morphological segregation and its relation to global parameters.

The results of our analysis suggest that different mechanisms control the morphological segregation depending on the galaxy environment. We find that mechanisms of a global nature dominate in high-density environments, namely, the virialized region of clusters, while local galaxy density as defined by Dressler (1980b) is the relevant parameter in the outskirts, where the influence of the cluster as a whole is relatively small compared with local effects.

As can be inferred from Figure 4, a primary parameter in the segregation of morphological types in high-density regions is the global cluster mass density at the position of the galaxies, computed using the scaling relationship between the mean cluster temperature and the projected NFW mass density profile. We find that the relative fraction of galaxy morphologies shows a stronger dependence on the local NFW projected density profile than on other radial distance normalizations such as r_{500} or r_{opt}. Therefore, these results might be applied to studies of other cluster galaxy properties that show a significant dependence on radial distance to the cluster centers, such as star formation rate and fraction of blue galaxies.

We conclude that the relative fraction of galaxy morphologies is more strongly correlated with the NFW (projected mass) profile than with the β-model (gas density) profile. This result may serve to assess the importance of tidal effects and gaseous phenomena operating in the transformation of spiral galaxies into S0's. Our results give support to the idea that tidal force effects produced by the cluster potential, galaxy harassment, or truncated star formation, among other physical mechanisms, would be primary in driving the observed morphological segregation in clusters of galaxies.

We have also taken into account different cluster properties in our analysis by considering subsamples of high and low cluster temperature and of high and low X-ray lumi-

nosity. The results of these analyses are similar to those obtained for the total sample, although in the high-density regions of hot clusters we find a tendency toward a stronger morphological segregation as a function of $\Sigma_{\rm mass}$.

This work was partially supported by the Consejo de Investigaciones Científicas y Técnicas de la Republica Argentina, CONICET, the Consejo de Investigaciones Científicas y Tecnológicas de la Provincia de Córdoba, CONICOR, and Fundación Antorchas, Argentina. We thank the referee for helpful suggestions.

APPENDIX

CORRECTIONS FOR BACKGROUND AND FOREGROUND GALAXIES AND MAGNITUDE CUTOFF

As extensively discussed by WGJ, corrections for background and foreground galaxies are to be applied when dealing with relative morphological fractions in clusters. For those computations requiring estimates of the local galaxy density, we have applied corrections in the same way as WGJ. We recall that the total mass density profile is obtained from the mean cluster temperatures of the intracluster gas, estimates of which are nearly free of projection effects.

However, estimates of the relative fractions of galaxy morphological types will be biased when a background/foreground galaxy is taken as a center to compute the corresponding gas or mass density. To correct for this effect, we have taken into account the correlation between galaxy projected density and the percentage of background/foreground galaxies given by WGJ. We estimate the corrections assuming a correlation between mass or gas density and the local galaxy density (see Fig. 3), which is a valid assumption given the small difference between observed and actual relative fractions of morphological types due to projection effects. Using the correlation found by WGJ between absolute magnitude and cumulative number of galaxies by morphological types, we have also corrected for absolute magnitude cutoff. This effect takes into account the fact that clusters with the same limiting apparent magnitude are at different distances.

REFERENCES

Abadi, M. G., Moore, B., & Bower, R. G. 1999, MNRAS, 308, 947
Barrow, J. D., Bhavsar, S. P., & Sonoda, D. H. 1984, MNRAS, 210, 19
Bartelmann, M. 1996, A&A, 313, 697
Byrd, G., & Valtonen, M. 1990, ApJ, 350, 89
Cowie, L. L., & Songaila, A. 1977, Nature, 266, 501
Dressler, A. 1980a, ApJS, 42, 565
———. 1980b, ApJ, 236, 351
Dressler, A., et al. 1997, ApJ, 490, 577 (D97)
Evrard A. E., Metzler, C. A., & Navarro, J. F. 1996, ApJ, 469, 494
Gunn, J. E., & Gott, J. R. 1972, ApJ, 176, 1
Jones, C., & Forman, W. 1999, ApJ, 511, 65
Lavery, R. J., & Henry, J. P. 1988, ApJ, 330, 596
Larson, R. B., Tinsley, B. M., & Caldwell, C. N. 1980, ApJ, 237, 692
Melnick, J., & Sargent, W. L. W. 1977, ApJ, 215, 401
Miller, R. H., 1988, Comments Astrophys., 13, 1
Moore, B., Katz, N., Lake, G., Dressler, A., & Oemler, A., Jr. 1996, Nature, 379, 613
Navarro, J. F., Frenk, C. S., & White, S. D. M. 1995, MNRAS, 275, 720 (NFW)
Oemler A., Jr. 1974, ApJ, 194, 1
Ostriker, J. P., & Tremaine, S. D., 1975, ApJ, 202, L113
Sanromà, M., & Salvador-Solé, E. 1990, ApJ, 360, 16
Valotto, C. A., Moore, B., & Lambas, D. G. 2001, ApJ, 546, 157
Whitmore, B. C., & Gilmore, D. M. 1991, ApJ, 367, 64
Whitmore, B. C., Gilmore, D. M., & Jones, C. 1993, ApJ, 407, 489 (WGJ)
Yee, H. K. C., Ellingson, E., & Carlberg, R. G. 1996, ApJS, 102, 269